Characterization and *Ex vivo* Evaluation of Curcumin Nanoethosomes for Melanoma treatment.

Rajesh Sreedharan Nair [a,b], Nashiru Billa [c,d], Lim Yang Mooi [e] and Andrew P. Morris [b,f]

[a] School of Pharmacy, Monash University Malaysia, Jalan Lagoon Selatan, 47500 Bandar Sunway, Selangor Darul Ehsan, Malaysia.

[b] School of Pharmacy, The University of Nottingham Malaysia, Jalan Broga, 43500 Semenyih, Selangor Darul Ehsan, Malaysia.

[c] College of Pharmacy, QU Health, Qatar University, Doha Qatar.

[d] Biomedical and Pharmaceutical Research Unit (BPRU), QU Health, Qatar University, Doha, Qatar.

[e] Centre for Cancer Research, Faculty of Medicine & Health Sciences, Universiti Tunku Abdul Rahman, LOT PT 21144, Jalan Sungai Long Bandar Sungai Long, Cheras, 43000 Kajang, Selangor.

[f] Swansea University Medical School, Swansea University, Singleton Park, Swansea, UK.

Running head: transdermal delivery of curcumin nanoethosomes

*****Corresponding author: Rajesh Sreedharan Nair
E mail : rajeshsreedharan.nair@monash.edu
Phone No: +60355146159
Fax : +60355146364

Abstract

This study aimed at developing curcumin nanoethosomes (Cur-Ets) with superior skin permeation intended for melanoma treatment. Although curcumin is active against many types of skin cancers, a suitable topical formulation is still lacking due to its hydrophobicity and poor skin permeation. The formulation was characterized using Scanning Transmission Electron Microscopy (STEM), atomic force microscopy (AFM), ATR-FTIR, DSC, and XRD. *In vitro* skin permeation was carried out using human skin, and the cytotoxicity of the formulation was evaluated on human melanoma cells (SK-MEL28). The vesicle size and zeta potential of the Cur-Ets were determined as 67 ± 1.6 nm and - 87.3 ± 3.3 mV, respectively. STEM and AFM analysis further support the size and morphology of the formulation. Curcumin's compatibility with formulation additives was confirmed by ATR-FTIR analysis. In addition, DSC and XRD analyses showed successful drug encapsulation in nanoethosomes. The drug encapsulation efficiency was determined as 87 ± 0.9%. The skin permeation of curcumin from Cur-Ets showed a superior flux (0.14 ± 0.03 µg cm^{-2} h^{-1}) compared to the control ($p< 0.05$). Cytotoxicity of the formulation demonstrated a time-dependent and concentration-dependent antiproliferative activity against melanoma cells. The developed Cur-Ets is suggested as a promising topical formulation for melanoma treatment.

Keywords: curcumin, melanoma, nanoethosomes, human skin, permeation, cytotoxicity.

Introduction

Skin cancer is the most prevalent type of cancer in the United States, and it is a major public health concern (Guy et al. 2015). Melanoma is a type of skin cancer that affects melanocytes and can appear wherever melanin is present. It accounts for only about 5% of all skin cancers, but in the United States, it is increasing at 5-8% every year. It is the most dangerous type of skin cancer and is extremely metastatic. The treatment option for melanoma includes surgical removal, radiation therapy, chemotherapy or cryotherapy (Chinembiri et al. 2014; Domingues et al. 2018). Many drugs are approved for treating melanomas; however, severe adverse effects associated with many chemotherapeutic drugs and multi-drug resistance are the causes of the low success rates. This necessitates the need for discovering new therapeutic agents with fewer side effects or enhancing the current technologies for safer and more effective therapy. It is known that the most challenging aspect of skin permeation is getting through the tough gateway, i.e. the stratum corneum (SC). Therefore, various permeation enhancement approaches such as chemical, physical or nano-carrier systems were widely employed. Nanoformulations can penetrate the outer layers of skin due to their smaller size and thereby facilitate the permeation of drug molecules (Zhou et al. 2018). Many strategies have been adopted for targeting drugs to skin cancers, and these include nanoparticles (Zhang et al. 2019), liposomes (Jose et al. 2018), ethosomes (Jalalpure et al. 2018), and micelles (Wang et al. 2020). Traditional liposomes appear only to permeate the upper layers of the stratum corneum rather than penetrating deep into the skin. Therefore, newer strategies such as ethosomes consisting of phospholipids and cholesterol with a relatively high ethanol content have shown promising skin permeation of several drugs (Bragagni et al. 2012). The high ethanol content in ethosomes may fluidise the SC lipids and enhance the skin permeation of drugs deeper into the skin layers.

Curcumin, a phenolic compound, commonly found in *Curcuma longa* Linn. (turmeric) (Naksuriya et al. 2014). The medicinal properties of turmeric are attributed mainly due to the presence of curcuminoids in the rhizome. Curcumin is one of three curcuminoids present in turmeric, and the amount varies between 2 and 5%, constitutes approximately 77% of the total curcuminoid content. The other two compounds are demethoxycurcumin (17-20%) and bis-demethoxycurcumin (5-10%). Studies report a range of pharmacological activities attributed to curcumin such as anti-inflammatory, anti-microbial, anti-oxidant, anticancer, and antidiabetic effects (Sun M et al. 2012). Although curcumin possesses wide pharmacological activities, its use as a medicinal agent is hindered due to its poor water solubility and instability (Vijayan et al. 2020).

Various nanotechnology-based delivery approaches such as nanoparticles (Adahoun et al. 2017), lipid vesicles (Yallapu et al. 2012), nano or microemulsions (Bergonzi et al. 2014; Sha et al. 2021), micelles (Kesharwani et al. 2015), polymeric conjugates (Pan et al. 2020), inclusion complexes (Sun Y et al. 2014) have been adopted in enhancing curcumin's efficacy. However, only a few promising studies for the topical delivery of this worthy drug, possibly due to its physico-chemical properties that control the passive diffusion through the skin layers. Curcumin-containing niosomes were found to have anticancer effects on breast cancer cell lines. This formulation, however, was not aimed for topical or transdermal delivery (Akbarzadeh et al. 2020). Furthermore, many reported studies have mainly utilised synthetic membranes, animal skin (Mangalathillam et al. 2012), or human cadaver skin (Pathan et al. 2018) to evaluate the permeation potential. These skin models may not correlate well with *in vivo* evaluations due to the physiological differences. Sun et al. developed in situ hydrogels containing curcumin-β-cyclodextrin inclusion complexes for melanoma treatment (Sun Y et al. 2014). The *in vitro* permeation through rat skin showed that curcumin from inclusion complexes was found to be higher than that from curcumin hydrogels, probably due

to the enhanced solubility and stability of curcumin in the inclusion complexes. Furthermore, an *in vitro* cytotoxicity study using mouse melanoma cell lines showed higher cytotoxicity with the formulation containing the curcumin inclusion complexes than with a curcumin solution. Although curcumin nanoformulations have shown some success in permeating through synthetic membranes and animal skin (Nair Rajesh Sreedharan et al. 2019; Soni et al. 2020), penetration remains a stumbling block when using full-thickness human skin. Reports suggest that ethosomes can permeate through the skin layers due to their superior deforming capacity, which could be beneficial in melanoma treatment (Yu et al. 2015; F et al. 2020). Pathan et al. report the anti-inflammatory effect of curcumin ethosomes utilising human cadaver skin for permeation evaluation support the feasibility of curcumin nanovesicles for deeper skin permeation (Pathan et al. 2018). Recently, Jalalpure et al. report the topical delivery of curcumin ethosomes for skin cancer and evaluated using excised rat skin (Jalalpure et al. 2018). The *in vitro* permeation study revealed an enhanced permeation and deeper skin deposition of curcumin compared to curcumin liposomes. Despite the fact that flux differ between rat and human skin, the study supports the efficacy of ethosomes over liposomes in the treatment of skin cancer. Although attempts are ongoing to enhance curcumin's topical delivery, studies aiming for melanoma using appropriate skin models are still lacking. Therefore, in this research, we have formulated highly deformable Cur-Ets aimed at melanoma treatment and evaluated the efficacy using a precise skin model, such as full-thickness human skin and their cytotoxicity in human melanoma cell lines.

Materials and Methods

Materials

Curcumin and cholesterol (>99%) were purchased from Sigma Aldrich, USA. Phosphatidylcholine (25%) from Soy Lecithin was purchased from MP Biomedicals, USA. Ethanol and acetonitrile (HPLC grade) were purchased from Fisher Scientific, UK. Eagle's

minimal essential medium (EMEM) was purchased from Cellgro® Mediatech Inc, USA. Polysorbate 80, foetal bovine serum and MTT reagent were purchased from Nacalai Tesque, Japan. The human melanoma cell line (SK-MEL-28) was obtained from the Center for Cancer Research, University Tunku Abdul Rahman (UTAR), Malaysia.

HPLC Method Development and Validation

Instrumentation and chromatographic conditions

For the method development, an Agilent HPLC 1290 Infinity system with an auto-injector and a Diode Array detector was used. A reverse-phase column (Hypersil Gold C18, 250 mm) maintained at 30 °C employing isocratic elution, and the wavelength was optimised at 425 nm. The method validation included linearity, precision, accuracy, limit of detection (LOD), limit of quantification (LOQ), and system suitability studies.

Linearity and range

Various solvents such as acetonitrile (AN), methanol, and acetic acid solution (AS) were initially tested at different compositions as mobile phase (Jayaprakasha et al. 2002). The final optimised mobile phase was a mixture of AN and AS (2.0% v/v) with selection being based on the best peak resolution, minimal peak tailing and shorter retention time. From the stock solution (1 mg/mL curcumin in methanol), a set of five different concentrations of curcumin, ranging between 2 and 10 µg/mL were prepared by diluting with methanol. From each dilution, 15 µL samples were then injected into the HPLC system, and the corresponding peak areas were noted. Linearity was assessed by plotting the area under the curve (AUC) against the concentration and examined the regression coefficient (R^2) values obtained on intra-day and inter-day (n=5) (Nair SR et al. 2021).

Precision and Accuracy

The precision and accuracy were determined on low, medium and high concentration samples of curcumin in the calibration range (n = 5), reported as relative standard deviation (% RSD) and percentage relative error (% RE) respectively (ICH 2005).

LOD and LOQ

ICH guidelines outline several approaches for the determination of LOD and LOQ, and we utilised the calibration curves. The calibration curves consisting of 5 different concentrations of curcumin were generated and the slope and intercept values were determined (n=5). The LOD and LOQ were calculated using the formulae (ICH 2005) :

$$\text{LOD} = \frac{3.3\,\sigma}{S}\text{ , LOQ} = \frac{10\,\sigma}{S}$$

Where, σ = standard deviation of the y-intercept of the regression lines, S = slope of the calibration curves.

System suitability studies

System suitability evaluations include capacity factor (k'), resolution (Rs), number of theoretical plates, tailing factor and signal to noise ratio (S/N) (Martins et al. 2017). For better peak separation and superior analysis, ICH recommends the following standards: a theoretical plate number of > 2000, k' and Rs > 2.0 and a peak tailing of < 2.0.

Formulation of curcumin nanoethosomes.

Nanoethosomes were developed by using the modified thin-film hydration technique (Zhai et al. 2015). Briefly, curcumin (1mg), soya phosphatidylcholine (SPC, 100 mg), cholesterol (10 mg), and tween 80 (10 mg) were taken in a round bottom (RB) flask (25 mL) and were dissolved in chloroform: methanol mixture (2:1). The organic solvents (Büchi Rotavapor R-200, Switzerland) evaporated by rotating the RB flask at 50 rpm for 30 minutes at 40˚C. The thin film deposited on the sides of the RB flask was then rehydrated using 10 mL aqueous ethanolic solution (40%v/v) by rotating for a further one hour. The dispersion containing

multilamellar vesicles was then sonicated using a probe sonicator (Q Sonica, Newtown, USA) at an amplitude of 20% for 60 Sec to obtain nanoethosomes of the desired size.

Particle size and zeta potential (ZP)

Zetasizer Nano ZS (Malvern Instruments, UK) was used to evaluate the ethosomal size and ZP (n = 3). The Cur-Ets were adequately diluted with deionised water (1:3) in a glass cuvette, and the mean vesicle size was measured (Karakucuk and Tort 2020). For ZP measurements, the undiluted sample was filled into a folded capillary zeta cell, and an average of 3 replicate scans was recorded. All the measurements were recorded at 25°C.

Surface morphology analysis

Surface morphology of Cur-Ets was studied using Scanning Transmission Electron Microscopy (STEM) and atomic force microscopy (AFM). Photomicrograph of the formulation was taken using a Field Emission Scanning Electron Microscope (Quanta 400F, FEI, USA) operated at a voltage of 5 kV and a magnification of 20000 X. Using a micropipette, a small amount of ethosomal suspension was spread on a copper grid and dried overnight at 25°C. The STEM images were captured for blank ethosomes and Cur-Ets. AFM analysis was performed using Bruker instrument (Bruker Crest, Model: Dimension edge) equipped with NanoScope analysis software version 1.7. The freshly prepared samples were diluted with deionized water (1:6), and a tiny drop was placed on a glass slide and air-dried at ambient temperature. The images were recorded using a silicone tip on nitride lever at a scan rate of 0.5 Hz.

Determination of the Encapsulation efficiency (EE)

The curcumin nanoethosomal formulation was kept overnight at 4 °C and centrifuged (Beckman Coulter, Allegra® 64R Centrifuge) at 25000 rpm at 4 °C for 45 minutes. The drug content in the supernatant was considered as the unentrapped portion. The total curcumin present in the formulation was determined after lysing the vesicles with Triton X (10%), and

the drug content was analysed using HPLC. The EE was calculated as reported earlier (Nair Rajesh Sreedharan et al. 2019).

$$\% \text{ EE} = \frac{\text{Total amount of curcumin in the formulation - Unentrapped curcumin}}{\text{Total amount of curcumin in the formulation}} \times 100$$

Attenuated Total Reflectance – Fourier Transform Infrared Spectroscopy (ATR-FTIR)

The drug-excipient compatibility was assessed using a Perkin-Elmer ATR-FTIR spectrophotometer. The sample holding crystal surface was cleaned using acetone to avoid any interference on the spectrum that arise from contaminants. Firstly, a background scan was run, and then a small amount of the freeze-dried sample was placed on the crystal surface and scanned between the band regions 4000- 400 cm^{-1} over 36 scans at a resolution of 4 cm^{-1}. The FTIR spectra were recorded for cholesterol, SPC, blank ethosomes, curcumin, Cur-Ets and compared with reference standards.

Differential Scanning Calorimetry (DSC)

DSC analysis was carried out using DSC Q2000 (TA Instruments, USA) which measures the endothermic and exothermic processes when the sample is heated, hence the thermal behaviour. Comparing the thermogram of pure curcumin with Cur-Ets allows the identification of changes in the physicochemical properties of curcumin after formulation. The freeze-dried Cur-Ets, SPC, cholesterol and pure curcumin were taken into a T- Zero aluminium pan and sealed with a T Zero aluminium lid where an empty pan was used as the reference. The sample was run from 0 to 300˚C at a heat rate of 10˚C/minute, and the thermogram was recorded.

X-ray diffraction (XRD) analysis

The diffractograms of curcumin and Cur-Ets were obtained using X'pert Pro X-ray diffractometer (Panalytical, Netherlands). The X-ray diffractometer is equipped with a Cu K-

alpha radiation source operated at 45 kV and 40 mA. The samples were scanned up to 70°. with a scanning speed of 0.02°/step and a step time of 0.5 sec.

Ex-vivo permeation studies of Cur-Ets using full-thickness human skin.

Prior to the permeation experiments, the institutional ethics approval was obtained from the University of Nottingham Malaysia (No:RS010516). Human skin was collected from a local hospital after obtaining written consent from patients who had undergone abdominoplasty. The subcutaneous fat was carefully removed, and the skin pieces (3 cm^2) were stored at −20 °C until future use. Franz diffusions cells having 0.95 cm^2 area with donor and receptor volumes of 1 mL and 2 mL respectively were used for the permeation studies (Singh et al. 2018; Jaipakdee et al. 2021). The excised human skin was conditioned by placing it in phosphate-buffered saline (PBS) for 30 minutes, positioned between the donor and receptor compartments (SC facing the donor), and tightened with a horseshoe clamp. The receptor compartment was filled with PBS containing tween 80 (1%w/v) as a solubilising agent and sodium azide (0.02% w/v) as an antibacterial. The temperature of the diffusion assembly was held at 37°C and it was equilibrated for 1 hour before the experiment began. The donor compartment was loaded with Cur-Ets (500 µg of curcumin) dispersed in acetate buffer pH5.0 (n=5). Samples from the receptor compartments were withdrawn (200 µL) at regular intervals up to 72 hours and analysed using the RP-HPLC method described earlier. After every sample collection, the same volume was replaced with fresh receptor fluid that helps maintain the sink condition. The cumulative permeation vs time profile was generated, and the flux was calculated from the linear portion of the graph (Rajesh and Sujith ; Nair R. S. and Nair 2015).

Cytotoxicity assay

Cytotoxicity of the formulation on human melanoma cell lines (SK-MEL28) was evaluated using MTT assay (Nair Rajesh Sreedharan et al. 2019). The cells were cultured in EMEM

medium supplemented with 10% foetal bovine serum and incubated at 37 °C in 5% CO_2. The fully confluent cells were harvested by treating with trypsin that detaches cells adhered to the culture flask. Thereafter, an equal volume of EMEM was added to the cell suspension and centrifuged at 1500 rpm for 5 minutes. The cell pellet was then dispersed in 1 mL of medium and diluted to the desired volume. The cells (5×10^3 cells/well) were seeded in a 96-well plate and incubated for about 24 hours to adhere the cells to the plates. After that, the medium was aspirated, and the cells were treated with curcumin solution, drug-free nanoethosome (blank), or Cur-Ets (2.5 - 10 µg/mL) after suitable dilution with serum-free EMEM medium. The untreated cells maintained at the same experimental conditions were the control. After the specified incubation (48-72hours), 20 µL of MTT solution (Stock concentration: 5mg/mL) was added to each well and further incubated for 4 hours. The supernatant was removed, and the violet coloured formazan crystals were solubilised by adding DMSO. The colour intensity was measured at 570 nm using a microplate reader (Biotek Instruments, Inc USA.) (n=4). The cytotoxicity and IC 50 values were calculated by comparing with the control.

Statistical analysis

The statistical analysis of data was done using the Graph-Pad Prism 8 software, and the results were presented as mean ± standard deviation. One-way ANOVA was used to assess statistical significance between groups, followed by Tukey's –HSD test, with $p < 0.05$ deemed statistically significant.

Results and Discussion

HPLC method development and validation

The mobile phase used for the curcumin analysis was optimised after many trials using different solvent compositions with the ultimate aim to obtain the best peak symmetry, high resolution, and a short run time. An optimal retention time and resolution were obtained with

the mobile phase composition of 45:55 (AN:AS) at a flow rate of 1.1 mL/min. A sharp peak of curcumin was observed at 10.4 minutes with an excellent peak symmetry (Figure 1).

Linearity

Excellent linearity was evident from the R^2 values of 0.9997 and 0.9999 for inter-day and intra-day linearity respectively. The linear range of detectability depends on the compounds analysed and the type of detector used; an R^2 value close to 1.0 indicates the best linearity. Low R^2 values can arise from errors in serial dilution, particularly when handling samples of very low concentrations (Jayaprakasha et al. 2002).

Accuracy and Precision

To investigate the accuracy and precision of the HPLC method; curcumin samples were analysed at high (10 μg/mL), medium (6 μg/mL) and low concentrations (2 μg/mL). The method demonstrates a low %RSD values (< 1.71%) confirm an excellent intra-day and inter-day precision (Table 1). The %RSD value < 2.0 is acceptable according to USP specifications and confirms that the method is sufficiently precise. The % RE values for both intra-day and inter-day accuracy was below 2.0% (Table 1). The low % RE confirmed the accuracy of the method.

Limits of detection and Limit of quantification

The LOD and LOQ of curcumin were determined as 0.12 μg/mL and 0.36 μg/mL, respectively. The lower detection with our method may be due to the choice of 425 nm as the ideal detection wavelength. Curcumin's absorption maxima were between 420 and 430 nm, as determined by an isoabsorbance plot produced with the chemstation software.

System suitability studies

At low, medium, and high curcumin concentrations, the system suitability parameters such as capacity factor, resolution, theoretical plates, peak symmetry, and signal to noise ratio (S/N) were determined. (Table 2). An excellent resolution above 2.0 and a capacity factor of >3.0

were seen for all the peaks corresponding to curcumin which satisfies the criteria for good separation. The theoretical plate number (N) was >13,000 for all the concentrations analysed. As expected, the S/N ratio increased as the concentration of the analyte increased. The tailing factor was found to be between 1.02 and 1.03. The accuracy of analysis decreases with the increase in peak tailing; a tailing factor close to 1.00 is considered optimal; however, a tailing factor of < 2.0 is acceptable (ICH 2005).

Formulation of curcumin nanoethosomes

Curcumin nanoethosome was successfully developed by film evaporation technique. We recently reported optimising drug-free nanoethosomes by altering the lipid concentration, ethanol content, and sonication time (Nair Rajesh Sreedharan et al. 2020). Furthermore, it is suggested that the nanosize particles are capable of transporting drugs across the skin layers; therefore, we aimed to limit the ethosomal size below 100 nm (Raju Y et al. 2017; Manickam et al. 2019). Particle size was found to increase with increasing concentrations of SPC and ethanol. Our report suggests that the blank ethosomes containing 1%w/w lipid (SPC) and 40% ethanol content demonstrated a homogeneous size distribution with PDI values below 0.25, and ethosomes size was found below 100 nm (Nair Rajesh Sreedharan et al. 2020). Therefore, we selected the optimized blank ethosomes containing 40% ethanol and 1%w/v SPC for incorporating curcumin in this study. The average vesicle size of the optimised curcumin nanoethosome (Cur-Ets) was found to be 67 ± 1.6 nm and ZP as -87.3 ± 3.3 mV. Sonication time and amplitude play a significant role in determining ethosome size and stability. Prolonged sonication at high amplitude may generate heat and can deteriorate the formulation. Hence, a lower amplitude (20%) and a short duration of 60 Sec were maintained for the formulation development. The ZP value influences the stability of vesicles, higher the ZP (+ve or –ve) greater the interparticle repulsion, and lesser aggregation (Tareen et al. 2020).

STEM and AFM analysis

STEM imaging was used to photograph the vesicles because SEM imaging was unable to provide consistent images. The Cur-Ets showed a spherical shape (Figure 2a), and no vesicle aggregation was observed, indicating a homogeneous distribution. AFM analysis further supports the morphology and surface texture of the formulation. The particle distribution was found to be homogeneous, which was evident from the 3D images, and the vesicles appeared sufficiently apart (Figure 2b).

Encapsulation efficiency

The EE of Cur-Ets was determined as 87 ± 0.9%. The centrifugation method has the advantage that it can be employed for measuring the entire drug that was encapsulated in the vesicles, which include the drug distributed in the lipid bilayer membrane and the drug encapsulated in the internal core. During the formulation process, some drug quantity may have been lost from the RB flask while removing the contents. Therefore, the total drug present in the formulation was determined by lysing the ethosomes using Triton-X and analysed using HPLC. Reports suggest that ethanol increases the EE of lipophilic drugs, probably due to the enhanced solubility of compounds in ethanol due to its co-solvent effect (Dubey et al. 2007).

FTIR analysis

The FTIR spectra of curcumin, SPC, cholesterol, and Cur-Ets are shown in Figure 3. Curcumin is a polyphenolic compound that showed principal peaks at 3506.9 cm^{-1} (phenolic O-H stretching), 1627.3 cm^{-1} (C=C stretching), 1504.9 cm^{-1} (−C=O and C=C vibrations), 1426.9 cm^{-1} and 1273.75 cm^{-1} correspondings to -olefinic C-H bending vibrations and aromatic C–O stretching respectively (Kolev et al. 2005). SPC consists of phosphoric acid, choline, phospholipids and showed characteristic peaks at 2923.0 cm^{-1} (CH_2 stretching vibration), 1736.6 cm^{-1} (carbonyl C=O stretching vibration), 1614.8 cm^{-1} (N−H bending of

primary amines), and 1460.7 cm^{-1} (C−H bending of CH_3). The spectrum for cholesterol showed a weak band at 3394.4 cm^{-1} (O−H stretching vibration) and 2930.5 cm^{-1} (CH_2 stretching vibration), peaks at 1462.5 cm^{-1} and 1364.9 cm^{-1} are −C−C− aromatic stretching and C−O stretching, respectively. The principal peaks of curcumin and additives were also seen in the spectra of the curcumin nanoethosome suggesting the drug-excipient compatibility and also warrants the successful incorporation of curcumin in the formulation.

DSC analysis

Figure 4 shows the thermogram of curcumin and other additives used in the formulation Cur-Ets. Since cholesterol and curcumin are crystalline, they have sharp endothermic peaks at 150.2 °C and 179.4 °C, which correspond to their melting points. These sharp peaks were not present in the blank or drug-loaded formulations that were consistent with previous research. (Wan et al. 2012). The disappearance of the endothermic peaks suggests the accommodation of drug molecules to the bilayer. Studies have shown a possible chemical bonding with the phenolic −OH group of curcumin and the polar head of phosphatidylcholine. Therefore, the intercalated drug molecules would have interfered with the spatial arrangement of the phospholipid (Chen et al. 2012; Tung et al. 2017). A relatively weak endothermic peak seen at 95.5 °C in the blank formulation was probably due to the melting of the freeze-dried ethosomes. A baseline shift towards a higher temperature may be due to the vaporisation of the samples as the heat capacity is directly linked to sample weight. Exothermic peaks observed in both blank and drug-loaded formulation beyond 250 °C were possibly due to the decomposition of the lipid materials.

XRD analysis

The XRD diffractogram of curcumin, formulated Cur-Ets are shown in figure 5. A typical XRD pattern shows the intensity of X-rays scattered at different angles by the sample and is usually recorded as counts/sec. The XRD diffractogram of curcumin showed many

characteristic sharp peaks at a series of scattering angles between 0° and 30° such as at 10.01°, 14.09°, 17.5°, 21.39°, 23.49°, 23.91°, 24.71°, 25.65°, 27.53° and 29.07° which were attributed to curcumin crystallinity. These characteristic peaks were diminished or suppressed in the formulation, suggesting the transformation of the crystalline structure of curcumin into a disordered crystalline or amorphous state. These results corroborate with similar previous reports suggesting that peak disappearance or a reduction in peak strength is due to the decreased crystallinity or amorphous nature of compounds. (Chereddy et al. 2013; Mahmood et al. 2018). The change in crystalline characteristics might have occurred during the synthesis of the ethosomes due to the intermolecular interactions between curcumin and other formulation additives. Overall, the FTIR, DSC, and XRD analyses reveal the intermolecular interaction of curcumin with the lipids suggesting a successful drug encapsulation.

Ex vivo permeation of curcumin nanoethosomes using full-thickness human skin

The cumulative curcumin permeated across the human skin from the formulation was 10.96 ± 1.6 µg cm^{-2} with a flux of 0.14 ± 0.03 µg cm^{-2} h^{-1}, which was significantly higher than the respective control, $p<0.05$ (Figure 6). The poor solubility of curcumin in the hydroalcoholic solution (control) may have been the limiting factor for permeation from the control. According to Akbari et al., transdermal delivery of curcumin niosomes improved the antinociceptive and anti-inflammatory effects in Wistar rats, and skin permeation studies across rat skin show superior skin deposition and permeation of niosomes compared to curcumin solution (Akbari et al. 2020). This further warrants the aptness of curcumin nanoformulations for topical or transdermal delivery. Elsayed et al. report a comparative permeation between encapsulated ethosomes and hydroalcoholic solutions containing the same ingredients; the drug permeation from the encapsulated ethosomes was higher than the hydroalcoholic solution (Elsayed et al. 2007). The Elsayed et al. report strengthens the argument for using drug-encapsulated ethosomes to increase transdermal permeation. The

nanosize and flexibility of ethosomal vesicles, together with the drug's inherent properties, would have been involved in promoting skin permeation. Ethosomes, being highly deformable, can penetrate the SC and subsequently fuse with skin lipids and release their encapsulated drug into the deeper layers of the skin. The passive diffusion of molecules is largely dependent on their molecular weight, and the log *P*. This was evident from the low permeation observed with gamma-tocotrienol (log *P* of 8.9 and MW 411 Da) in our recent report (Nair Rajesh Sreedharan et al. 2020). Curcumin has a more favourable log *P* (3.3) and MW (368 Da) compared to gamma-tocotrienol; therefore, it can permeate easily through the lipophilic-hydrophilic regions. In contrast, the highly lipophilic gamma-T3 may diffuse slower through the relatively hydrophilic dermis layer. Although the exact mechanism of ethosomes for enhanced skin permeation is unclear, there could involve a synergistic mechanism between the phospholipid and ethanol. Ethanol is a proven permeation enhancer and can disrupt the lipid packing of SC so that the flexible ethosomes can penetrate and traverse deeper into the skin layers. Furthermore, the phospholipid present in ethosomes would have interacted with the SC lipids and can alter the lipid transition temperature leading to enhanced membrane permeability (Yang et al. 2017).

Cytotoxicity study on human melanoma cell lines

The cytotoxicity of curcumin solution, blank nanoethosomes, and Cur-Ets was evaluated on melanoma (SK-MEL28) cell lines (Figure 7). The skin permeation studies have demonstrated that curcumin from the nanoethosomal formulation efficiently permeated through the full-thickness human skin, and this would be beneficial in melanoma treatment (Yu et al. 2015). Nanoformulations can passively target cancer cells due to their enhanced permeability and retention (EPR) effect (Naves et al. 2017). As a result of leaky vasculature and the poor lymphatic drainage of tumor tissues, nanoformulations can easily enter the tumor site and remain within. The cytotoxicity of curcumin and Cur-Ets was tested at concentrations

between 2.5 and 10 µg/mL. This concentration range was set after testing each drug solution for a wide range of concentrations. The cell viability (%) was calculated compared to the untreated cells at the same experimental conditions. The drug solutions and the formulations showed a concentration-dependent and time-dependent antiproliferative activity. Cur-Ets demonstrated a significant reduction in the cell viability (<20%) of SK-MEL-28 cell lines at the higher curcumin concentration (10 µg/mL). It was promising that the observed cell viability after treatment with Cur-Ets was comparable to pure curcumin solutions. This showed that the nanoethosome formulation process did not appear to have adversely affected the pharmacological activity of curcumin. The IC_{50} values of curcumin and Cur-Ets at the 48-hour incubation point were 6.9 and 7.2 µg/mL respectively (p=0.997) whereas, the corresponding IC_{50} values at 72-hours were 6.3 and 5.5 µg/mL respectively (p=0.168). There was no significant difference in IC_{50} seen between the two sets. The comparable IC_{50} values of the drug and the formulation suggest their parallel cytotoxic potential. These results suggest that Cur-Ets may have a place in melanoma treatment.

Conclusion

Cur-Ets were successfully formulated and evaluated *in vitro* for potential topical application against melanoma. The smaller ethosomal size is ideal for enhanced skin permeation, and the colloidal stability is ensured by its high negative ZP. The ATR-FTIR analysis warrants curcumin's compatibility with formulation additives. Furthermore, DSC and XRD investigations indicate that the nanoethosomes were successfully formed, as evidenced by high encapsulation efficiency. Interestingly, the skin permeation of curcumin from Cur-Ets showed superior transdermal flux to that of the control solution ($p < 0.05$), suggesting the efficacy of ethosomal formulation. Cytotoxicity studies of the formulations on human melanoma cells showed promising antiproliferative activity, which warrants its potential use in melanoma treatment. Overall, the Cur-Ets developed in this study fulfill the essential

requirements for the topical application against melanoma. Further *in vivo* evaluations are required to substantiate these findings.

Conflict of Interest

The authors report no declarations of interest.

Acknowledgements

The authors would like to express their gratitude to the Faculty of Science, University of Nottingham Malaysia for the financial assistance given to this research project.

References

Adahoun MaA, Al-Akhras M-AH, Jaafar MS, Bououdina M. 2017. Enhanced anti-cancer and antimicrobial activities of curcumin nanoparticles. Artificial Cells, Nanomedicine, and Biotechnology. 45(1):98-107.

Akbari J, Saeedi M, Enayatifard R, Morteza-Semnani K, Hassan Hashemi SM, Babaei A, Rahimnia SM, Rostamkalaei SS, Nokhodchi A. 2020. Curcumin Niosomes (curcusomes) as an alternative to conventional vehicles: A potential for efficient dermal delivery. Journal of Drug Delivery Science and Technology. 60:102035.

Akbarzadeh I, Tavakkoli Yaraki M, Ahmadi S, Chiani M, Nourouzian D. 2020. Folic acid-functionalized niosomal nanoparticles for selective dual-drug delivery into breast cancer cells: An in-vitro investigation. Advanced Powder Technology. 31(9):4064-4071.

Bergonzi MC, Hamdouch R, Mazzacuva F, Isacchi B, Bilia AR. 2014. Optimization, characterization and in vitro evaluation of curcumin microemulsions. LWT - Food Science and Technology. 59(1):148-155.

Bragagni M, Mennini N, Maestrelli F, Cirri M, Mura P. 2012. Comparative study of liposomes, transfersomes and ethosomes as carriers for improving topical delivery of celecoxib. Drug Delivery. 19(7):354-361.

Chen Y, Wu Q, Zhang Z, Yuan L, Liu X, Zhou L. 2012. Preparation of Curcumin-Loaded Liposomes and Evaluation of Their Skin Permeation and Pharmacodynamics. Molecules. 17(5):5972-5987.

Chereddy KK, Coco R, Memvanga PB, Ucakar B, des Rieux A, Vandermeulen G, Preat V. 2013. Combined effect of PLGA and curcumin on wound healing activity. Journal of Control Release. 171(2):208-215.

Chinembiri T, du Plessis L, Gerber M, Hamman J, du Plessis J. 2014. Review of Natural Compounds for Potential Skin Cancer Treatment. Molecules. 19(8):11679-11721.

Domingues B, Lopes JM, Soares P, Pópulo H. 2018. Melanoma treatment in review. Immunotargets Ther. 7:35-49. eng.

Dubey V, Mishra D, Dutta T, Nahar M, Saraf D, Jain N. 2007. Dermal and transdermal delivery of an anti-psoriatic agent via ethanolic liposomes. Journal of Controlled Release. 123(2):148-154.

Elsayed MMA, Abdallah OY, Naggar VF, Khalafallah NM. 2007. Lipid vesicles for skin delivery of drugs: Reviewing three decades of research. International Journal of Pharmaceutics. 332(1):1-16.

F AG, Sayed OM, Abo El-Ela FI, Kharshoum RM, Salem HF. 2020. Treatment of Basal Cell Carcinoma Via Binary Ethosomes of Vismodegib: In Vitro and In Vivo Studies. AAPS PharmSciTech. 21(2):51.

Guy GP, Machlin SR, Ekwueme DU, Yabroff KR. 2015. Prevalence and Costs of Skin Cancer Treatment in the U.S., 2002−2006 and 2007−2011. American Journal of Preventive Medicine. 48(2):183-187.

ICH. 2005. Validation of analytical procedures: text and methodology Q2(R1). [accessed 16 May 2019]. https://www.fda.gov/regulatory-information/search-fda-guidance-documents/international-council-harmonisation-ich-guidance-documents.
Jaipakdee N, Jarukamjorn K, Putalun W, Limpongsa E. 2021. Permeation, stability and acute dermal irritation of miroestrol and deoxymiroestrol from Pueraria candollei var. mirifica crude extract loaded transdermal gels. Pharmaceutical development and technology. 26(9):967-977.
Jalalpure SS, Kumbar VM, Patil SR, Joshi SA, Bhat KG, Diwan PV. 2018. Factorial design based curcumin ethosomal nanocarriers for the skin cancer delivery: In vitro evaluation Journal of Liposome Research.1-21.
Jayaprakasha GK, Jagan Mohan Rao L, Sakariah KK. 2002. Improved HPLC method for the determination of curcumin, demethoxycurcumin, and bisdemethoxycurcumin. Journal of Agricultural and Food Chemistry. 50(13):3668-3672.
Jose A, Labala S, Ninave KM, Gade SK, Venuganti VVK. 2018. Effective Skin Cancer Treatment by Topical Co-delivery of Curcumin and STAT3 siRNA Using Cationic Liposomes. AAPS PharmSciTech. 19(1):166-175.
Karakucuk A, Tort S. 2020. Preparation, characterization and antimicrobial activity evaluation of electrospun PCL nanofiber composites of resveratrol nanocrystals. Pharmaceutical development and technology. 25(10):1216-1225.
Kesharwani P, Banerjee S, Padhye S, Sarkar FH, Iyer AK. 2015. Parenterally administrable nano-micelles of 3,4-difluorobenzylidene curcumin for treating pancreatic cancer. Colloids and Surfaces B: Biointerfaces. 132:138-145.
Kolev TM, Velcheva EA, Stamboliyska BA, Spiteller M. 2005. DFT and experimental studies of the structure and vibrational spectra of curcumin. International Journal of Quantum Chemistry. 102(6):1069-1079.
Mahmood S, Mandal UK, Chatterjee B. 2018. Transdermal delivery of raloxifene HCl via ethosomal system: Formulation, advanced characterizations and pharmacokinetic evaluation. International Journal of Pharmaceutics. 542(1-2):36-46.
Mangalathillam S, Rejinold NS, Nair A, Lakshmanan VK, Nair SV, Jayakumar R. 2012. Curcumin loaded chitin nanogels for skin cancer treatment via the transdermal route. Nanoscale. 4(1):239-250. eng.
Manickam B, Sreedharan R, Chidambaram K. 2019. Drug/Vehicle Impacts and Formulation Centered Stratagems for Enhanced Transdermal Drug Permeation, Controlled Release and Safety: Unparalleled Past and Recent Innovations-An Overview. Current Drug Therapy. 14(3):192-209.
Martins LG, khalil NM, Mainardes RM. 2017. Application of a validated HPLC-PDA method for the determination of melatonin content and its release from poly(lactic acid) nanoparticles. Journal of Pharmaceutical Analysis. 7(6):388-393.
Nair RS, Billa N, Leong C-O, Morris AP. 2020. An Evaluation of Tocotrienol Ethosomes for Transdermal Delivery using Strat-M® membrane and excised Human skin. Pharmaceutical development and technology.1-29.
Nair RS, Morris A, Billa N, Leong C-O. 2019. An Evaluation of Curcumin-Encapsulated Chitosan Nanoparticles for Transdermal Delivery [journal article]. AAPS PharmSciTech. 20(2):69.
Nair RS, Nair S. 2015. Permeation Studies of Captopril Transdermal Films Through Human Cadaver Skin. Curr Drug Deliv. 12(5):517-523. eng.
Nair SR, Billa N, Morris A. 2021. A Validated Reverse-Phase High Performance Liquid Chromatography (RP-HPLC) Method for the Quantification of Gamma- Tocotrienol in Tocotrienol Rich Fractions of Crude Palm Oil. Current Nutrition & Food Science. 17:1-7.
Naksuriya O, Okonogi S, Schiffelers RM, Hennink WE. 2014. Curcumin nanoformulations: a review of pharmaceutical properties and preclinical studies and clinical data related to cancer treatment. Biomaterials. 35(10):3365-3383.
Naves LB, Dhand C, Venugopal JR, Rajamani L, Ramakrishna S, Almeida L. 2017. Nanotechnology for the treatment of melanoma skin cancer. Progress in Biomaterials. 6(1-2):13-26.

Pan R, Zeng Y, Liu G, Wei Y, Xu Y, Tao L. 2020. Curcumin–polymer conjugates with dynamic boronic acid ester linkages for selective killing of cancer cells. Polymer Chemistry. 11(7):1321-1326.
Pathan IB, Jaware BP, Shelke S, Ambekar W. 2018. Curcumin loaded ethosomes for transdermal application: Formulation, optimization, in-vitro and in-vivo study. Journal of Drug Delivery Science and Technology. 44:49-57.
Rajesh S, Sujith S. Permeation of Flurbiprofen polymeric films through human cadaver skin.
Raju Y P, Chowdary V H, Nair RS, Basha D J. 2017. In vitro assessment of non-irritant microemulsified voriconazole hydrogel system. Artificial Cells, Nanomedicine, and Biotechnology. 45(8):1539-1547.
Sha K, Ma Q, Veroniaina H, Qi X, Qin J, Wu Z. 2021. Formulation optimization of solid self-microemulsifying pellets for enhanced oral bioavailability of curcumin. Pharmaceutical development and technology. 26(5):549-558.
Singh I, Nair RS, Gan S, Cheong V, Morris A. 2018. An evaluation of crude palm oil (CPO) and tocotrienol rich fraction (TRF) of palm oil as percutaneous permeation enhancers using full-thickness human skin. Pharmaceutical development and technology. 24(4):448-454.
Soni K, Mujtaba A, Akhter MH, Zafar A, Kohli K. 2020. Optimisation of ethosomal nanogel for topical nano-CUR and sulphoraphane delivery in effective skin cancer therapy. Journal of microencapsulation. 37(2):91-108.
Sun M, Su X, Ding B, He X, Liu X, Yu A, Lou H, Zhai G. 2012. Advances in nanotechnology-based delivery systems for curcumin. Nanomedicine. 7(7):1085-1100.
Sun Y, Du L, Liu Y, Li X, Li M, Jin Y, Qian X. 2014. Transdermal delivery of the in situ hydrogels of curcumin and its inclusion complexes of hydroxypropyl-β-cyclodextrin for melanoma treatment. International Journal of Pharmaceutics. 469(1):31-39.
Tareen FK, Shah KU, Ahmad N, Asim.ur.Rehman, Shah SU, Ullah N. 2020. Proniosomes as a carrier system for transdermal delivery of clozapine. Drug Dev Ind Pharm. 46(6):946-954.
Tung BT, Hai NT, Son PK. 2017. Hepatoprotective effect of Phytosome Curcumin against paracetamol-induced liver toxicity in mice. Brazilian Journal of Pharmaceutical Sciences. 53(1):1-13.
Vijayan UK, Varakumar S, Sole S, Singhal RS. 2020. Enhancement of loading and oral bioavailability of curcumin loaded self-microemulsifying lipid carriers using Curcuma oleoresins. Drug Dev Ind Pharm. 46(6):889-898.
Wan S, Sun Y, Qi X, Tan F. 2012. Improved Bioavailability of Poorly Water-Soluble Drug Curcumin in Cellulose Acetate Solid Dispersion [journal article]. AAPS PharmSciTech. 13(1):159-166.
Wang M-Z, Niu J, Ma H-J, Dad HA, Shao H-T, Yuan T-J, Peng L-H. 2020. Transdermal siRNA delivery by pH-switchable micelles with targeting effect suppress skin melanoma progression. Journal of Controlled Release.
Yallapu MM, Jaggi M, Chauhan SC. 2012. Curcumin nanoformulations: a future nanomedicine for cancer. Drug discovery today. 17(1):71-80.
Yang L, Wu L, Wu D, Shi D, Wang T, Zhu X. 2017. Mechanism of transdermal permeation promotion of lipophilic drugs by ethosomes. International Journal of Nanomedicine. 12:3357-3364.
Yu X, Du L, Li Y, Fu G, Jin Y. 2015. Improved anti-melanoma effect of a transdermal mitoxantrone ethosome gel. Biomedicine & Pharmacotherapy. 73:6-11.
Zhai Y, Xu R, Wang Y, Liu J, Wang Z, Zhai G. 2015. Ethosomes for skin delivery of ropivacaine: preparation, characterization and ex vivo penetration properties. Journal of Liposome Research. 25(4):316-324.
Zhang Y, Bush X, Yan B, Chen JA. 2019. Gemcitabine nanoparticles promote antitumor immunity against melanoma. Biomaterials. 189:48-59.
Zhou X, Hao Y, Yuan L, Pradhan S, Shrestha K, Pradhan O, Liu H, Li W. 2018. Nano-formulations for transdermal drug delivery: A review. Chinese Chemical Letters. 29(12):1713-1724.

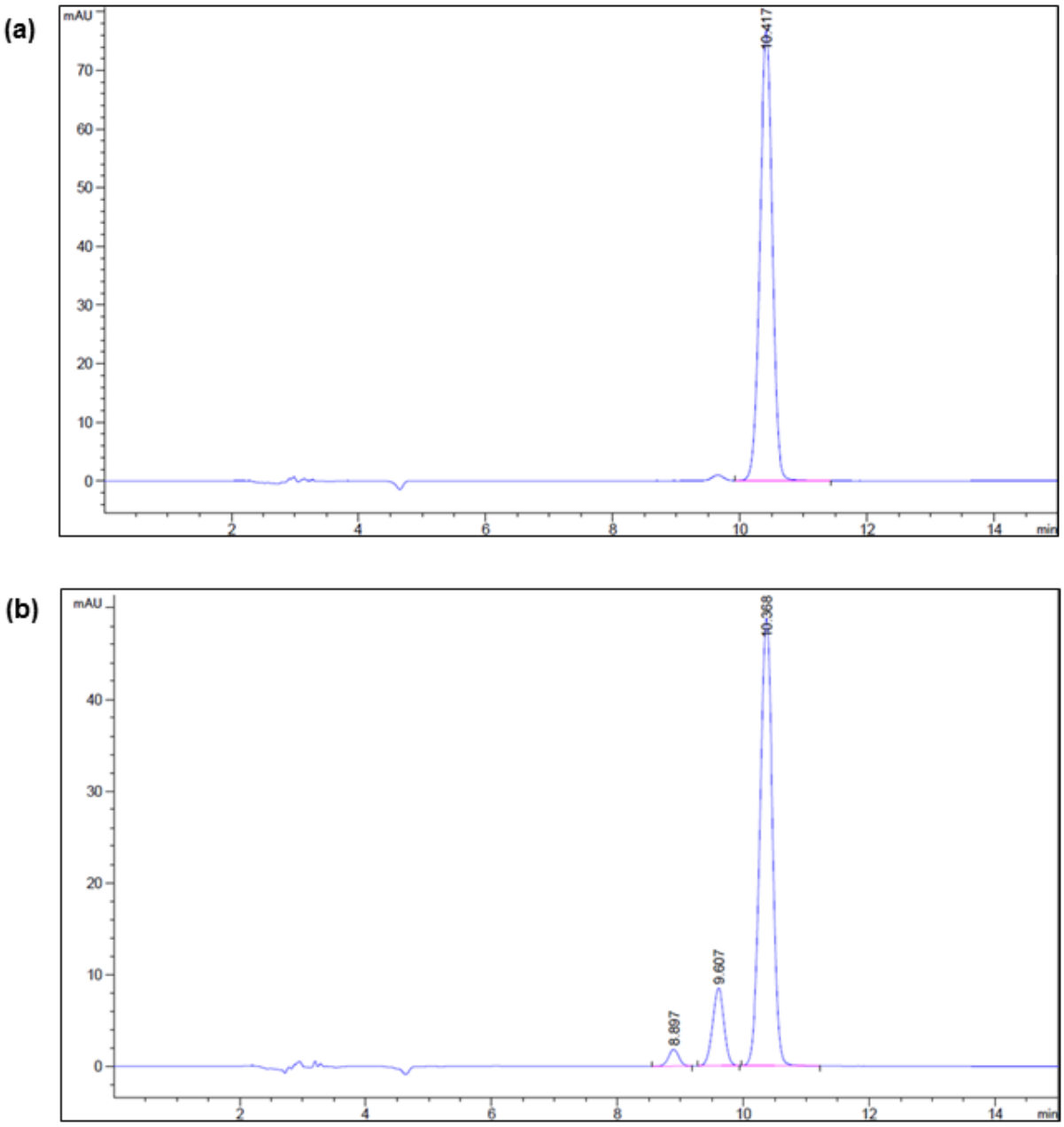

Figure 1. HPLC chromatogram showing the retention time of curcumin at 10.4 minutes (a) analytical standard, (b) curcuminoids.

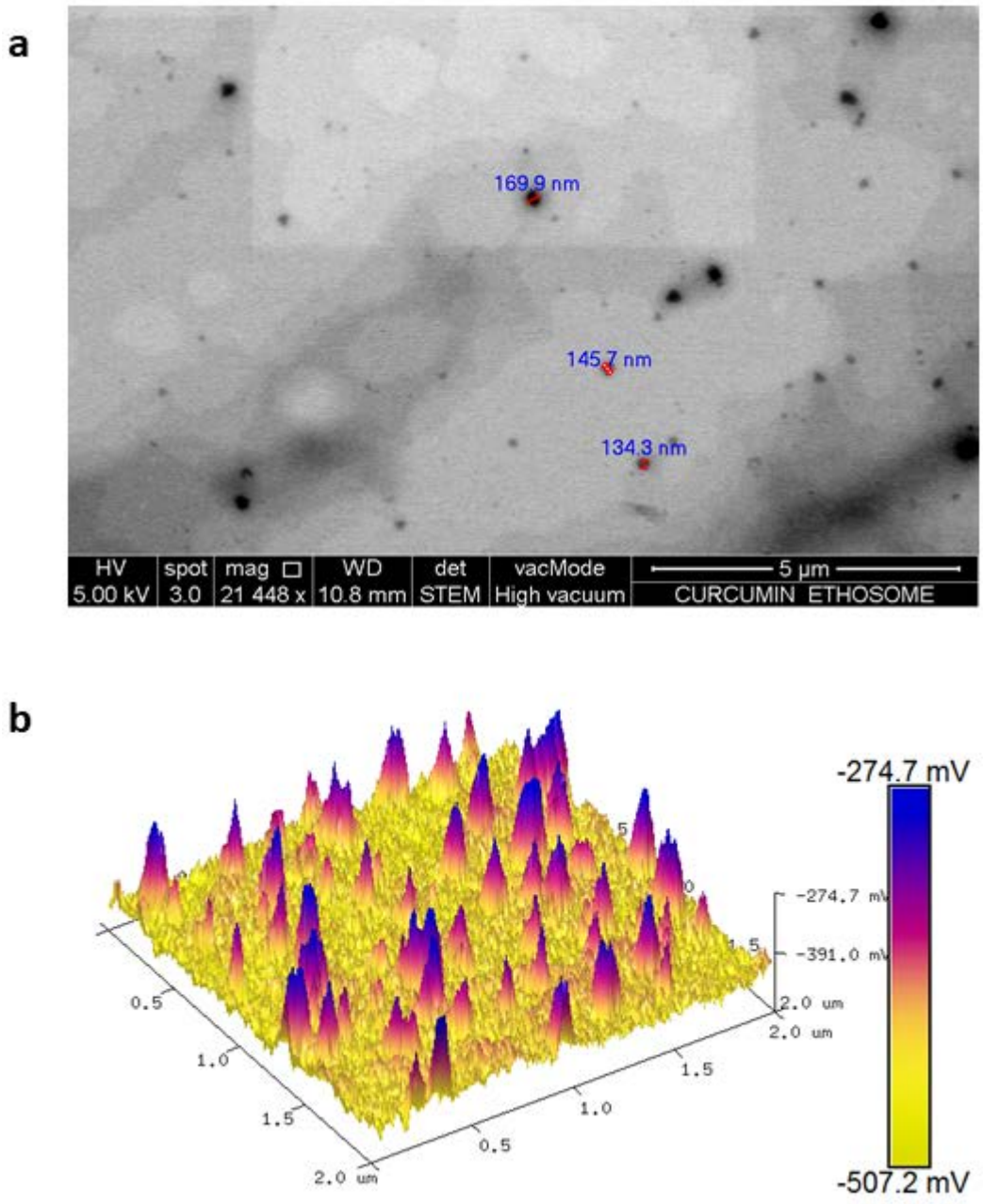

Figure 2. STEM images of curcumin curcumin nanoethosomes at 20,000 x magnification (a), and AFM images showing vesicle distribution and the structure in the 3D plane (b).

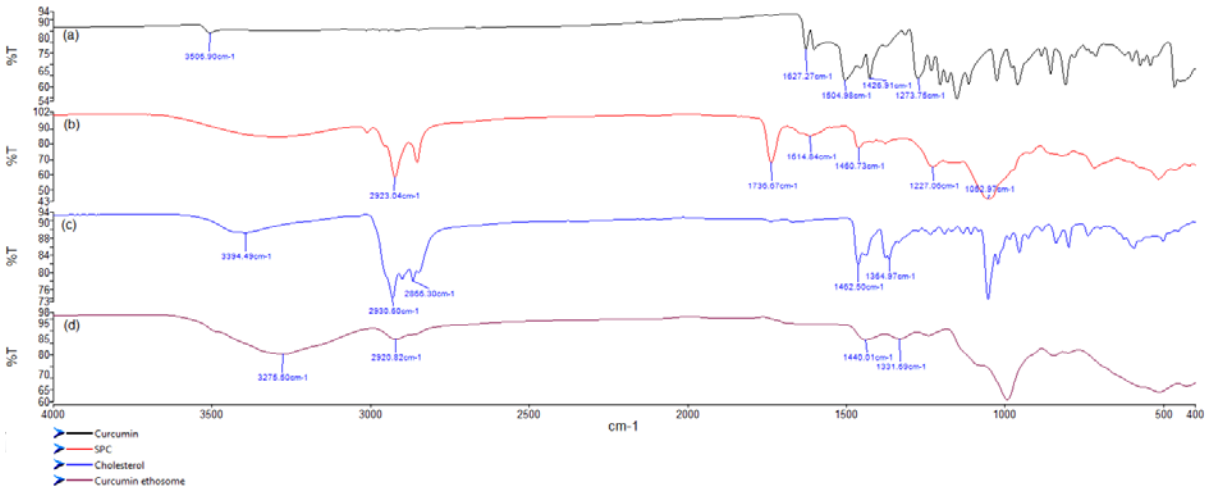

Figure 3. FTIR spectra of soya phosphatidylcholine (SPC), cholesterol, curcumin and curcumin nanoethosomes.

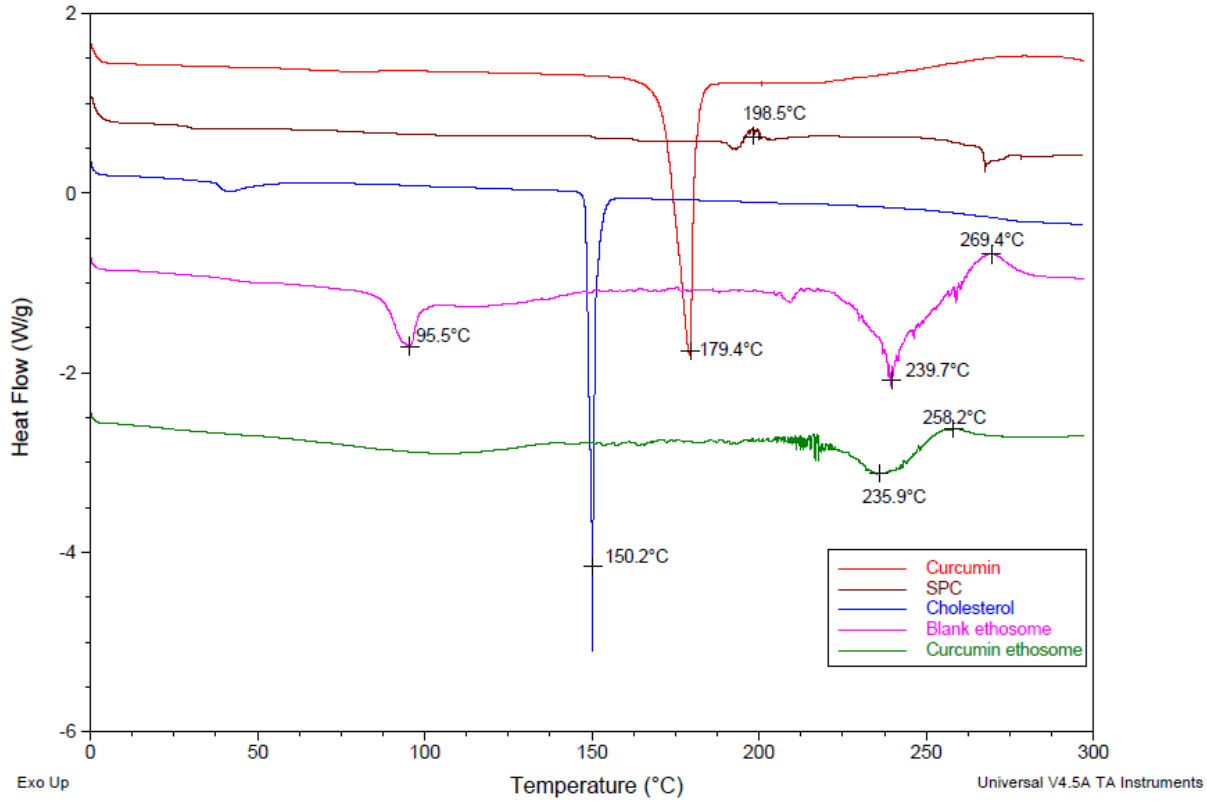

Figure 4. DSC thermogram of curcumin, soya phosphatidylcholine (SPC), cholesterol, blank nanoethosomes and the curcumin nanoethosomes.

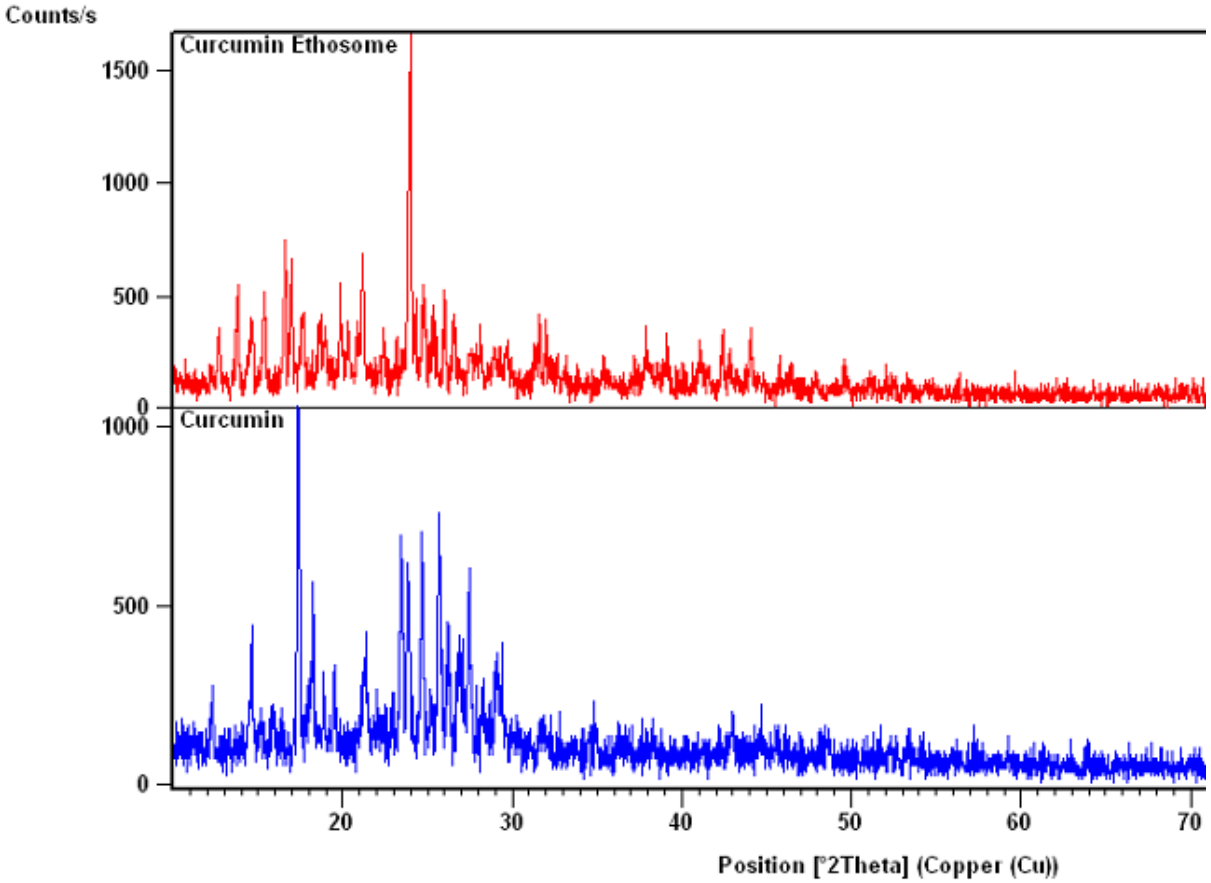

Figure 5. XRD diffractogram of curcumin and curcumin nanoethosomes.

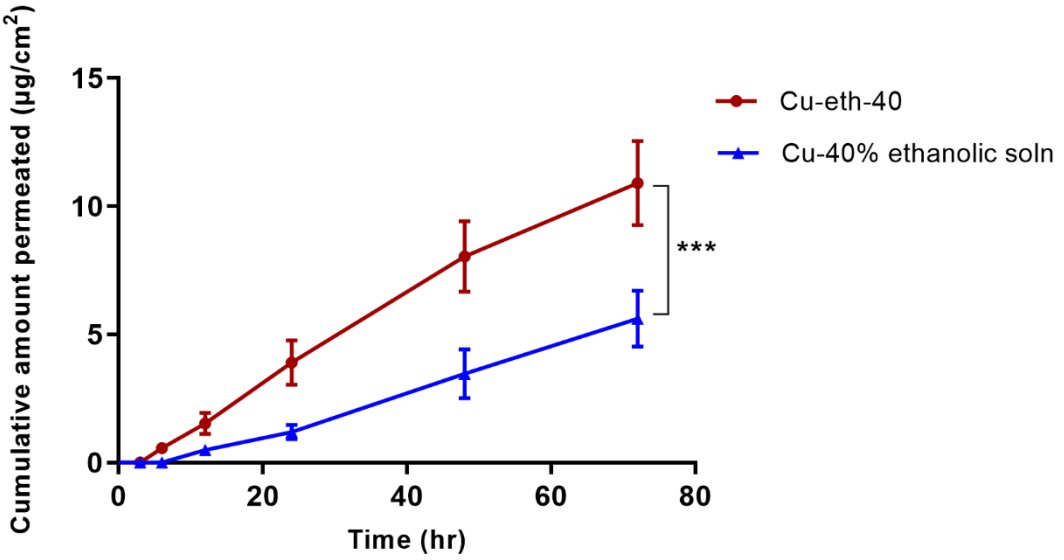

Figure 6. Permeation of curcumin from nanoethosomes containing 40% ethanol (Cueth-40) and control (curcumin in 40% ethanolic solution) through excised full-thickness human skin. Mean ± SD, n=5 (*** $p < 0.001$).

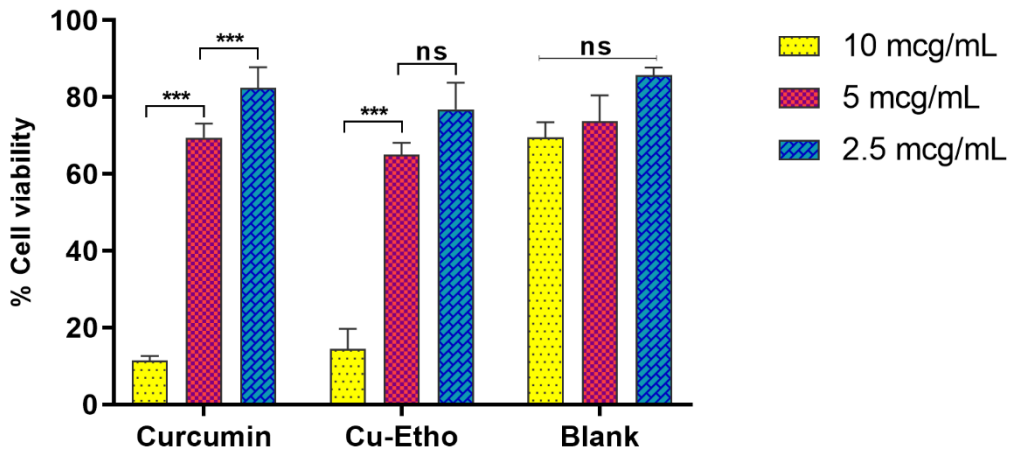

Figure 7. Percentage cell viability of melanoma cells on treatment with curcumin solution, blank nanoethosomes and curcumin nanoethosomes (Cu-Etho) at three different concentrations (2.5 µg/mL, 5 µg/mL, 10 µg/mL) after 72 h treatment. Mean ± SD, n=3. (***$p < 0.001$, ns- not significant).

Table .1 Precision and accuracy of low, medium and high concentration samples of curcumin on intra-day and inter-day (n=5).

Concentration (µg/mL)	Intra-day		Inter-day	
	Precision (% RSD)	Accuracy (%RE)	Precision (% RSD)	Accuracy (%RE)
2	1.01	-2.00%	1.54	-1.00 %
6	0.79	-1.17%	1.48	0.83%
10	1.43	0.80%	1.71	0.50%

RSD – relative standard deviation, RE- relative error

Table .2 System suitability studies at low, medium and high concentration samples of curcumin (n=5).

Concentration (µg/mL)	Capacity factor (k')	Resolution (R_s)	Theoretical plates (N)	Tailing factor (T)	S/N ratio
2	3.63 ± 0.02	2.20 ± 0.03	13290.67 ± 223.37	1.03 ± 0.01	302.20 ± 41.54
6	3.63 ± 0.02	2.18 ± 0.04	13382.00 ± 205.03	1.02 ± 0.01	1075.70 ± 82.78
10	3.66 ± 0.05	2.16 ± 0.03	13244.66 ± 216.60	1.02 ± 0.01	1467.07 ±120.44

S/N – signal to noise ratio